

# Capturing static and dynamic correlation with $\Delta$ NO-MP2 and $\Delta$ NO-CCSD

Cite as: J. Chem. Phys. **152**, 014101 (2020); <https://doi.org/10.1063/1.5140669>

Submitted: 29 November 2019 . Accepted: 09 December 2019 . Published Online: 02 January 2020

Joshua W. Hollett , and Pierre-François Loos 



View Online



Export Citation



CrossMark



Lock-in Amplifiers

Zurich Instruments

Watch the Video 

# Capturing static and dynamic correlation with $\Delta$ NO-MP2 and $\Delta$ NO-CCSD

Cite as: J. Chem. Phys. 152, 014101 (2020); doi: 10.1063/1.5140669

Submitted: 29 November 2019 • Accepted: 9 December 2019 •

Published Online: 2 January 2020



View Online



Export Citation



CrossMark

Joshua W. Hollett<sup>1,2,3,a)</sup>  and Pierre-François Loos<sup>3</sup> 

## AFFILIATIONS

<sup>1</sup>Department of Chemistry, University of Winnipeg, Winnipeg, Manitoba R3B 2G3, Canada

<sup>2</sup>Department of Chemistry, University of Manitoba, Winnipeg, Manitoba R3T 2N2, Canada

<sup>3</sup>Laboratoire de Chimie et Physique Quantiques (UMR 5626), Université de Toulouse, CNRS, UPS, Toulouse, France

<sup>a)</sup> Author to whom correspondence should be addressed: [j.hollett@uwinnipeg.ca](mailto:j.hollett@uwinnipeg.ca)

## ABSTRACT

The  $\Delta$ NO method for static correlation is combined with second-order Møller-Plesset perturbation theory (MP2) and coupled-cluster singles and doubles (CCSD) to account for dynamic correlation. The MP2 and CCSD expressions are adapted from finite-temperature CCSD, which includes orbital occupancies and vacancies, and expanded orbital summations. Correlation is partitioned with the aid of damping factors incorporated into the MP2 and CCSD residual equations. Potential energy curves for a selection of diatomics are in good agreement with extrapolated full configuration interaction results and on par with conventional multireference approaches.

Published under license by AIP Publishing. <https://doi.org/10.1063/1.5140669>

## I. INTRODUCTION

The correlation problem persists. To state it simply, how does one adequately account for electron correlation with a minimal amount of effort? Its persistence is ensured by the latter condition. This continual search for an efficient treatment of electron correlation is driven by the need to treat larger and more complex systems with increased accuracy. A common strategy of potential solutions is the partitioning of the problem into different types of correlation: static and dynamic,<sup>1–11</sup> long-range and short-range,<sup>12–16</sup> etc. Partitioning the correlation problem into static and dynamic correlation, strong and weak correlation, multireference and “the rest” is a popular and effective strategy that generally provides a qualitative, and sometimes quantitative, model for particularly challenging electronic structure problems. The price of the success of such models is relatively expensive calculations, often combined with the nontrivial definition of active spaces that requires both chemical intuition and trial-and-error. Through the reformulation of these problems in terms of alternative models of electronic structure, a deeper and more “physical” understanding of correlation partitioning can be achieved while providing another tool for the study of complex multireference systems.

A two-tiered wave function based approach to static and dynamic correlation is a relatively old idea.<sup>17–21</sup> The general strategy of manually (or automatically<sup>22,23</sup>) defining an active space, optimizing a multireference wave function, and then applying some form of post-Hartree-Fock electron correlation method is the basis of a multitude of multireference electronic structure models.<sup>21,24–26</sup> These models have continually evolved over the decades, and prominently include CASPT2,<sup>19,27,28</sup> NEVPT,<sup>29–31</sup> MRCC,<sup>17,18,32,33</sup> and NOCI.<sup>34–37</sup> These methods are essentially the default for studying systems with low-lying excited states (e.g., conical intersections), largely because conventional density functional methods often fail to properly model such systems. An emerging alternative to these approaches, particularly for describing the multireference aspect, is cumulant functional methods [e.g., density-matrix functional theory (DMFT)<sup>38–45</sup> and natural orbital functional theory (NOFT)<sup>46–53</sup>]. Recently, a two-tiered approach as seen in wave function approaches was devised for NOFT by Piris, NOF-MP2.<sup>53,54</sup> Other than NOF-MP2, the combination of a cumulant functional for static correlation and post-Hartree-Fock theories for dynamic correlation is unexplored.

Upon its inception, the  $\Delta$ NO method<sup>8</sup> involved employing a cumulant functional to account for static correlation (or multireference character) in conjunction with an on-top density

functional for dynamic correlation. The on-top density functional is applied directly to the statically correlated  $\Delta$ NO two-electron density matrix (2-RDM); therefore, the method for treating dynamic correlation can be easily substituted. Recently, multiple formulations of finite-temperature coupled-cluster approximations have been introduced,<sup>55,56</sup> including coupled-cluster singles and doubles (FT-CCSD)<sup>57</sup> by White and Chan, which is similar to thermal cluster cumulant theory.<sup>58–60</sup> In such an approach, orbitals are thermally populated according to a Fermi-Dirac distribution; therefore, there are noninteger electron occupancies and vacancies (holes). Similar formulations also exist for second-order Møller-Plesset perturbation theory (FT-MP2).<sup>60–62</sup> The finite-temperature formulations of post-Hartree-Fock approaches present an ideal framework for treating the dynamic correlation of a multireference (or statically correlated) 2-RDM obtained from  $\Delta$ NO or elsewhere.

The method presented here involves combining  $\Delta$ NO for static correlation with MP2 or CCSD for dynamic correlation, by exploiting aspects of the finite-temperature formulation. The combination is made possible by introducing a  $\Delta$ -dependent damping factor in the leading term of the MP2 or CCSD residuals, which modifies the occupancy-occupancy, vacancy-vacancy, and occupancy-vacancy pairs according to the amount of static correlation present. The  $\Delta$ NO method is introduced in Subsection II A, the modified MP2 and CCSD equations are described in Subsections II C and II B, and the damping factors are defined in the Appendix. The implementation of the method is described in Sec. III, and results for the dissociation of some diatomics are presented and discussed in Sec. IV. Finally, some conclusions regarding the current implementation and some future directions are discussed in Sec. V. Atomic units are used throughout unless stated otherwise.

## II. THEORY

### A. $\Delta$ NO method

Cumulant functional theory (CFT) is based on the cumulant expansion of the exact two-electron reduced density matrix (2-RDM) in terms of the one-electron reduced density matrix (1-RDM) and occasionally other variables.<sup>63</sup> The 2-RDM can be defined in terms of the  $N$ -electron wave function,

$$\tilde{\Gamma}(\mathbf{x}_1, \mathbf{x}_2, \mathbf{x}'_1, \mathbf{x}'_2) = \frac{N(N-1)}{2} \int \Psi^*(\mathbf{x}'_1, \mathbf{x}'_2, \mathbf{x}_3, \dots, \mathbf{x}_N) \times \Psi(\mathbf{x}_1, \mathbf{x}_2, \mathbf{x}_3, \dots, \mathbf{x}_N) d\mathbf{x}_3 \dots d\mathbf{x}_N, \quad (1)$$

where  $\mathbf{x} = (\mathbf{r}, \omega)$  represents both the spatial and spin coordinates of an electron. The 1-RDM follows from the 2-RDM via integration of the coordinates of one of the electrons,

$$\tilde{\gamma}(\mathbf{x}, \mathbf{x}') = \frac{2}{N-1} \int \tilde{\Gamma}(\mathbf{x}, \mathbf{x}_2, \mathbf{x}', \mathbf{x}_2) d\mathbf{x}_2. \quad (2)$$

The cumulant expansion of the 2-RDM can be written as

$$\tilde{\Gamma}(\mathbf{x}_1, \mathbf{x}_2, \mathbf{x}'_1, \mathbf{x}'_2) = \tilde{\Gamma}^{(0)}(\mathbf{x}_1, \mathbf{x}_2, \mathbf{x}'_1, \mathbf{x}'_2) + \tilde{\Gamma}_{\text{cum}}(\mathbf{x}_1, \mathbf{x}_2, \mathbf{x}'_1, \mathbf{x}'_2), \quad (3)$$

where the zeroth-order term of the expansion,  $\tilde{\Gamma}^{(0)}$ , is expressed solely in terms of the 1-RDM,

$$\tilde{\Gamma}^{(0)}(\mathbf{x}_1, \mathbf{x}_2, \mathbf{x}'_1, \mathbf{x}'_2) = \frac{1}{2} [\tilde{\gamma}(\mathbf{x}_1, \mathbf{x}'_1) \tilde{\gamma}(\mathbf{x}_2, \mathbf{x}'_2) - \tilde{\gamma}(\mathbf{x}_1, \mathbf{x}'_2) \tilde{\gamma}(\mathbf{x}_2, \mathbf{x}'_1)]. \quad (4)$$

The general form of the cumulant,  $\tilde{\Gamma}_{\text{cum}}$ , for an  $N$ -electron system is unknown, and present CFT methods are distinguished by how they approximate this term. When  $\tilde{\Gamma}_{\text{cum}}$  is constructed exclusively from the natural orbitals (NOs),  $\{\phi_p\}$ , and their occupancies,  $\{n_p\}$  (which are the eigenfunctions and eigenvalues of the 1-RDM, respectively), a natural orbital functional (NOF) is the result. For notational convenience, we also define natural vacancies as  $h_p = 1 - n_p$  and assume real-valued NOs. Unlike NOFs, the  $\Delta$ NO method uses electron transfer variables,  $\{\Delta_{me}\}$ , which correspond to the amount of electron occupancy transferred from an “occupied” active orbital  $\phi_m$  to a “virtual” active orbital  $\phi_e$ . Note that “occupied” and “virtual” designations refer to the ground-state Hartree-Fock electron configuration<sup>8</sup> (see Table I for orbital labeling).

In  $\Delta$ NO, the occupancies are defined in terms of these variational  $\{\Delta_{me}\}$ ,

$$n_m = 1 - \sum_e \Delta_{me}, \quad n_e = \sum_m \Delta_{me}. \quad (5)$$

Further distinguishing the  $\Delta$ NO functional from NOFs, or other cumulant functionals, is that the transfer of electrons occurs between a relatively small set of active occupied,  $\mathcal{A}_o = \{\phi_m\}$ , and virtual,  $\mathcal{A}_v = \{\phi_e\}$ , orbitals. This is because the  $\Delta$ NO cumulant functional is designed to capture only static correlation.

For this work, it is useful to describe the spinless, spin-resolved,  $\Delta$ NO 2-RDM. In general, the spinless 2-RDM is obtained by integrating over the spin of the two electrons,

$$\Gamma(\mathbf{r}_1, \mathbf{r}_2, \mathbf{r}'_1, \mathbf{r}'_2) = \iint \tilde{\Gamma}(\mathbf{x}_1, \mathbf{x}_2, \mathbf{x}'_1, \mathbf{x}'_2) \Big|_{\omega'_1=\omega_1}^{\omega'_1=\omega_1} \Big|_{\omega'_2=\omega_2}^{\omega'_2=\omega_2} d\omega_1 d\omega_2. \quad (6)$$

The result can then be resolved into the components associated with different spin-pairs,

$$\Gamma(\mathbf{r}_1, \mathbf{r}_2, \mathbf{r}'_1, \mathbf{r}'_2) = \Gamma^{\uparrow\uparrow}(\mathbf{r}_1, \mathbf{r}_2, \mathbf{r}'_1, \mathbf{r}'_2) + \Gamma^{\downarrow\downarrow}(\mathbf{r}_1, \mathbf{r}_2, \mathbf{r}'_1, \mathbf{r}'_2) + \Gamma^{\uparrow\downarrow}(\mathbf{r}_1, \mathbf{r}_2, \mathbf{r}'_1, \mathbf{r}'_2) + \Gamma^{\downarrow\uparrow}(\mathbf{r}_1, \mathbf{r}_2, \mathbf{r}'_1, \mathbf{r}'_2). \quad (7)$$

TABLE I. Orbital index key for  $\Delta$ NO, MP2, and CCSD.

Indices	Orbitals	Trait	Set label
$p, q, r, s$	All		
$i, j, k, l$	Occupied	$n_i \neq 0$	$\mathcal{O}$
$a, b, c, d$	Virtual	$h_a \neq 0$	$\mathcal{V}$
$m, n$	Active occupied	$n_m < 1$	$\mathcal{A}_o$
$e, f$	Active virtual	$h_e < 1$	$\mathcal{A}_v$

Furthermore, the 2-RDM can also be expanded in the basis of the NOs,

$$\Gamma(\mathbf{r}_1, \mathbf{r}_2, \mathbf{r}'_1, \mathbf{r}'_2) = \sum_{pqrs} \Gamma_{pqrs} \phi_p(\mathbf{r}'_1) \phi_q(\mathbf{r}'_2) \phi_r(\mathbf{r}_1) \phi_s(\mathbf{r}_2). \quad (8)$$

For a closed-shell system, the zeroth-order term of the cumulant expansion becomes

$$\left(\Gamma^{(0),\sigma\sigma}\right)_{pqrs} = \frac{n_p n_q}{2} \delta_{pr}^{qs}, \quad (9a)$$

$$\left(\Gamma^{(0),\sigma\sigma'}\right)_{pqrs} = \frac{n_p n_q}{2} \delta_{pr} \delta_{qs}, \quad (9b)$$

where  $\delta_{pr}^{qs} = \delta_{pr} \delta_{qs} - \delta_{ps} \delta_{qr}$ ,  $n_p = n_p^\uparrow = n_p^\downarrow$ , and  $\sigma, \sigma' = \uparrow$  or  $\downarrow$ .

The  $\Delta$ NO cumulant consists of three terms,

$$\Gamma_{\text{cum}}^{\Delta\text{NO}} = \Gamma_{\text{pair}}^{\Delta\text{NO}} + \Gamma_{\text{stat}}^{\Delta\text{NO}} + \Gamma_{\text{HSC}}^{\Delta\text{NO}}, \quad (10)$$

a pair correction term,  $\Gamma_{\text{pair}}^{\Delta\text{NO}}$ ; a static correlation term,  $\Gamma_{\text{stat}}^{\Delta\text{NO}}$ ; and a high-spin correction term,  $\Gamma_{\text{HSC}}^{\Delta\text{NO}}$ , where each can be decomposed into its spin-pair components.

For noninteger occupancies,  $\Gamma^{(0)}$  [see Eq. (9)] does not integrate to the total number of electron pairs,  $N(N-1)/2$ . The pair correction term,  $\Gamma_{\text{pair}}^{\Delta\text{NO}}$ , ensures that the total 2-RDM integrates to this number for any  $\{\Delta_{me}\}$  and is given as

$$\left(\Gamma_{\text{pair}}^{\Delta\text{NO},\sigma\sigma}\right)_{pqrs} = \frac{\Delta_{pq}(n_q - n_p - \Delta_{pq}) - \eta_{pq}}{2} \delta_{pr}^{qs}, \quad (11a)$$

$$\left(\Gamma_{\text{pair}}^{\Delta\text{NO},\sigma\sigma'}\right)_{pqrs} = \frac{n_p h_p}{2} \delta_{pq} \delta_{pr} \delta_{qs} + \frac{\Delta_{pq}(n_q - n_p - \Delta_{pq}) - \eta_{pq}}{2} \delta_{pr} \delta_{qs}, \quad (11b)$$

where

$$\eta_{pq} = \begin{cases} \sum_r \Delta_{pr} \Delta_{qr}, & \text{if } p \neq q \wedge (\phi_p, \phi_q) \in \mathcal{A}_o \\ \text{or } p \neq q \wedge (\phi_p, \phi_q) \in \mathcal{A}_v, \\ 0, & \text{otherwise,} \end{cases} \quad (12)$$

and  $\Delta_{pq} = -\Delta_{qp}$ .

In the framework of  $\Delta$ NO, static correlation is captured by transferring opposite-spin electron pairs from the same active occupied NO,  $\phi_m$ , to the same active virtual NO,  $\phi_e$ . This recovers the same intrapair correlation as the  $2n$ -tuple excitations of a seniority-zero configuration interaction wave function,<sup>64,65</sup> for which excitations are performed only within a relatively small active space.

The static correlation term of the cumulant is written as

$$\left(\Gamma_{\text{stat}}^{\Delta\text{NO},\sigma\sigma}\right)_{pqrs} = 0, \quad (13a)$$

$$\left(\Gamma_{\text{stat}}^{\Delta\text{NO},\sigma\sigma'}\right)_{pqrs} = \frac{\zeta_{pr} - \tau_{pr}}{2} \delta_{pq} \delta_{rs}, \quad (13b)$$

where

$$\zeta_{pq} = \begin{cases} \sum_r \sqrt{\Delta_{pr} \Delta_{qr}}, & \text{if } p \neq q \wedge (\phi_p, \phi_q) \in \mathcal{A}_o \\ \text{or } p \neq q \wedge (\phi_p, \phi_q) \in \mathcal{A}_v, \\ 0, & \text{otherwise,} \end{cases} \quad (14)$$

and

$$\tau_{pq} = \begin{cases} \sqrt{n_p \Delta_{pq}}, & \text{if } \phi_p \in \mathcal{A}_o \wedge \phi_q \in \mathcal{A}_v, \\ \sqrt{n_q \Delta_{qp}}, & \text{if } \phi_p \in \mathcal{A}_v \wedge \phi_q \in \mathcal{A}_o, \\ 0, & \text{otherwise.} \end{cases} \quad (15)$$

Like a seniority-zero wave function, no parallel-spin correlation is included in the static correlation term. However, the high-spin correction (HSC) includes interpair, opposite-spin and parallel-spin, correlation that is not present in a seniority-zero wave function. This correlation is necessary for the proper dissociation of multiple bonds into high-spin fragments and for the static correlation of multiple electron pairs in general.<sup>43</sup> The HSC term is written as

$$\left(\Gamma_{\text{HSC}}^{\Delta\text{NO},\sigma\sigma}\right)_{pqrs} = \frac{\kappa_{pq}}{2} \delta_{pr}^{qs}, \quad (16a)$$

$$\left(\Gamma_{\text{HSC}}^{\Delta\text{NO},\sigma\sigma'}\right)_{pqrs} = -\frac{\kappa_{pq}}{2} \delta_{pr} \delta_{qs}, \quad (16b)$$

where

$$\kappa_{pq} = \begin{cases} \sum_{\substack{r \neq s \\ (r \neq q) \\ (s \neq p)}} \tau_{pr} \tau_{qs}, & \text{if } p \neq q \wedge (\phi_p, \phi_q) \in \mathcal{A}, \\ 0, & \text{otherwise.} \end{cases} \quad (17)$$

The HSC reduces the pair density between opposite-spin electrons, while increasing the pair density between parallel-spin electrons, of separate statically correlated electron pairs, as their static correlation increases. This is illustrated in Fig. 1 for two statically correlated electron pairs. Taking  $\text{N}_2$  dissociation as an example, the HSC ensures that the spin-up electrons of each of the three statically correlated pairs (triple bond) simultaneously appear on one atom, while the spin-down electrons appear on the other, resulting in a superposition of the two high-spin fragment possibilities. Without the correction, the electrons of each statically correlated pair would encounter an average of both parallel and opposite-spin electrons from the other statically correlated pairs (i.e., spin-averaged).

The total  $\Delta$ NO energy follows simply from the 2-RDM,

$$E^{\Delta\text{NO}} = E^{(0)} + E_{\text{cum}}^{\Delta\text{NO}}, \quad (18)$$

where the zeroth-order 1-RDM energy also includes the one-electron, kinetic, and electron-nucleus attraction energy in addition

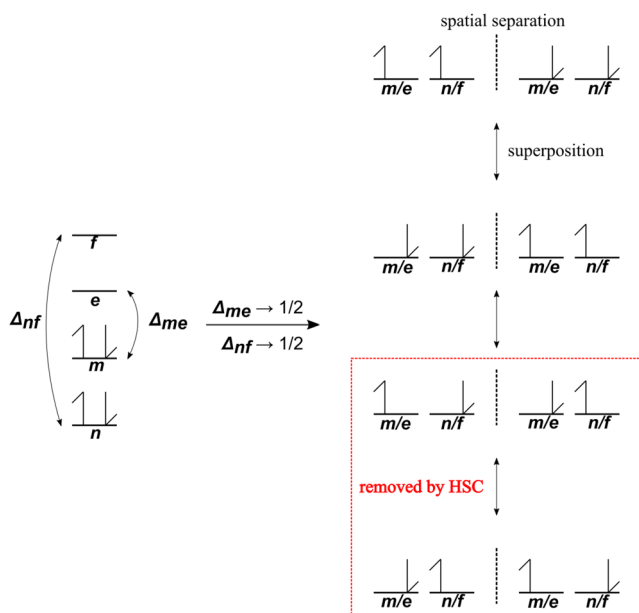


**FIG. 1.** Diagrammatic representation of the  $\Delta$ NO high-spin correction (HSC) for two statically correlated electron pairs. Without the HSC, at complete static correlation ( $\Delta = 1/2$ ), the  $\Delta$ NO 2-RDM would contain a superposition of four different spin configurations about a spatial separation (dashed line) (e.g., dissociated atoms). The HSC removes the “low-spin” configurations, leaving only the “high-spin” configurations.

to the two-electron energy associated with the zeroth-order term of the cumulant expansion,  $\Gamma^{(0)}$ . For a closed-shell system, the zeroth-order 1-RDM energy, in terms of NOs and occupancies, is given as

$$E^{(0)} = 2 \sum_p n_p H_p + \sum_{pq} n_p n_q (2J_{pq} - K_{pq}), \quad (19)$$

where

$$H_p = \int \phi_p(\mathbf{r}) \left( -\frac{\nabla^2}{2} - \sum_A \frac{Z_A}{r_A} \right) \phi_p(\mathbf{r}) d\mathbf{r}, \quad (20a)$$

$$J_{pq} = \iint \frac{\phi_p(\mathbf{r}_1)\phi_q(\mathbf{r}_2)\phi_p(\mathbf{r}_1)\phi_q(\mathbf{r}_2)}{r_{12}} d\mathbf{r}_1 d\mathbf{r}_2, \quad (20b)$$

$$K_{pq} = \iint \frac{\phi_p(\mathbf{r}_1)\phi_q(\mathbf{r}_2)\phi_q(\mathbf{r}_1)\phi_p(\mathbf{r}_2)}{r_{12}} d\mathbf{r}_1 d\mathbf{r}_2 \quad (20c)$$

are the usual one-electron (kinetic and nuclear attraction) and two-electron (Coulomb and exchange) integrals over NOs. The cumulant energy is given as

$$E_{\text{cum}}^{\Delta\text{NO}} = E_{\text{pair}}^{\Delta\text{NO}} + E_{\text{stat}}^{\Delta\text{NO}} + E_{\text{HSC}}^{\Delta\text{NO}} + E_{\text{dyn}}^{\Delta\text{NO}}, \quad (21)$$

with components defined as follows:

$$E_{\text{pair}}^{\Delta\text{NO}} = \sum_p n_p h_p J_{pp} + \sum_{pq} \Delta_{pq} (n_q - n_p - \Delta_{pq}) (2J_{pq} - K_{pq}) - \sum_{pq} \eta_{pq} (2J_{pq} - K_{pq}), \quad (22a)$$

$$E_{\text{stat}}^{\Delta\text{NO}} = \sum_{pq} (\zeta_{pq} - \tau_{pq}) L_{pq}, \quad (22b)$$

$$E_{\text{HSC}}^{\Delta\text{NO}} = - \sum_{pq} \kappa_{pq} K_{pq}, \quad (22c)$$

where the time-inversion exchange energy integrals are

$$L_{pq} = \iint \frac{\phi_p(\mathbf{r}_1)\phi_p(\mathbf{r}_2)\phi_q(\mathbf{r}_1)\phi_q(\mathbf{r}_2)}{r_{12}} d\mathbf{r}_1 d\mathbf{r}_2. \quad (23)$$

The HSC energy appears simplified in comparison with the 2-RDM term [see Eq. (16)]. This is because the Coulomb repulsion terms cancel due to the equivalence of the spin-up and spin-down NOs. The dynamic correlation energy,  $E_{\text{dyn}}^{\Delta\text{NO}}$ , was defined previously in terms of an on-top density functional.<sup>8</sup> In the present study, the dynamic correlation energy is provided via MP2 or CCSD, i.e.,

$$E_{\text{dyn}}^{\Delta\text{NO}} = E_{\text{MP2/CCSD}}^{\Delta\text{NO}}. \quad (24)$$

## B. CCSD for $\Delta$ NO

Recently, White and Chan introduced a finite-temperature formulation of the coupled-cluster singles and doubles (FT-CCSD) method.<sup>57</sup> The method is formulated in terms of imaginary time, which is integrated from 0 to  $\beta$ , where  $\beta$  is the inverse temperature. The authors state that at zero temperature, the FT-CCSD amplitudes, and consequently the energy, converge to the usual nontemperature dependent CCSD values. In that case, the electron occupancies, which are determined by a Fermi-Dirac distribution, would collapse to their normal Aufbau (Hartree-Fock ground state) values. For  $\Delta$ NO, the occupancies are not those of Aufbau or the Fermi-Dirac distribution; nevertheless, it is assumed here that aspects of the FT-CCSD formulation are still valid. In their article, White and Chan outline how to convert CC equations (i.e., residuals) to FT-CC equations. The equations presented here are formulated by taking the CCSD equations of Stanton *et al.*<sup>66</sup> and applying the instructions from White and Chan to include occupancies and vacancies (holes). The necessary instructions (paraphrased) are as follows: (i) for each contraction, sum over all orbitals instead of just occupied or virtual orbitals and (ii) include an occupancy or vacancy with each index not associated with an amplitude. Application of these instructions to the residual ( $r_i^a$  and  $r_{ij}^{ab}$ ) equations of Stanton *et al.* gives

$$r_i^a(\text{CCSD}) = n_i h_a s_i^a F_{ia} + \sum_c t_i^c \mathcal{F}_{ac} - \sum_k t_k^a \mathcal{F}_{ki} + \sum_{kc} t_{ik}^{ac} \mathcal{F}_{kc} - \sum_{kc} t_k^c \langle ka || ic \rangle n_i h_a - \frac{1}{2} \sum_{kcd} t_{ik}^{cd} \langle ka || cd \rangle h_a - \frac{1}{2} \sum_{klc} t_{kl}^{ac} \langle lk || ci \rangle n_i \quad (25)$$

and

$$r_{ij}^{ab}(\text{CCSD}) = n_i n_j h_a h_b d_{ij}^{ab} \langle ij || ab \rangle + P_{ab} \sum_c t_{ij}^{ac} \left( \mathcal{F}_{bc} - \frac{1}{2} \sum_k t_k^b \mathcal{F}_{kc} \right) - P_{ij} \sum_k t_{ik}^{ab} \left( \mathcal{F}_{kj} + \frac{1}{2} \sum_c t_j^c \mathcal{F}_{kc} \right) + \frac{1}{2} \sum_{kl} \tau_{kl}^{ab} \mathcal{W}_{klj} + \frac{1}{2} \sum_{cd} \tau_{ij}^{cd} \mathcal{W}_{abcd} + P_{ij} P_{ab} \sum_{kc} \left( t_{ik}^{ac} \mathcal{W}_{kbcj} - t_i^c t_k^a \langle kb || cj \rangle h_b n_j \right) + P_{ij} \sum_c t_i^c \langle ab || cj \rangle n_j h_a h_b - P_{ab} \sum_k t_k^a \langle kb || ij \rangle n_i n_j h_b, \quad (26)$$

where  $P$  is a permutation operator such that  $P_{ij} g_{ij} = g_{ji}$ . The various matrix elements from Eqs. (25) and (26) read

$$\mathcal{F}_{ac} = h_a F_{ac} - \frac{1}{2} \sum_k t_k^a F_{kc} + \sum_{kd} t_k^d \langle ka || dc \rangle h_a - \frac{1}{2} \sum_{kld} \tilde{\tau}_{kl}^{ad} \langle kl || cd \rangle, \quad (27a)$$

$$\mathcal{F}_{ki} = n_i F_{ik} + \frac{1}{2} \sum_c t_i^c F_{kc} + \sum_{cl} t_l^c \langle kl || ic \rangle n_i + \frac{1}{2} \sum_{lcd} \tilde{\tau}_{il}^{cd} \langle kl || cd \rangle, \quad (27b)$$

$$\mathcal{F}_{kc} = F_{kc} + \sum_{ld} t_l^d \langle kl || cd \rangle \quad (27c)$$

and

$$\mathcal{W}_{klj} = n_i n_j \langle kl || ij \rangle + P_{ij} \sum_c t_j^c \langle kl || ic \rangle n_i + \frac{1}{4} \sum_{cd} \tau_{ij}^{cd} \langle kl || cd \rangle, \quad (28a)$$

$$\mathcal{W}_{abcd} = h_a h_b \langle ab || cd \rangle - P_{ab} \sum_k t_k^b \langle ak || cd \rangle h_a + \frac{1}{4} \sum_{kl} \tau_{kl}^{ab} \langle kl || cd \rangle, \quad (28b)$$

$$\mathcal{W}_{kbcj} = h_b n_j \langle kb || cj \rangle + \sum_d t_j^d \langle kb || cd \rangle h_b - \sum_l t_l^b \langle kl || cj \rangle n_j - \sum_{ld} \left( \frac{t_{jl}^{db}}{2} + t_j^d t_l^b \right) \langle kl || cd \rangle, \quad (28c)$$

where we have defined the intermediate quantities

$$\tilde{\tau}_{ij}^{ab} = t_{ij}^{ab} + t_i^a t_j^b - t_i^b t_j^a, \quad (29a)$$

$$\tilde{\tau}_{ij}^{ab} = t_{ij}^{ab} + \frac{1}{2} \left( t_i^a t_j^b - t_i^b t_j^a \right). \quad (29b)$$

The element

$$F_{pq} = \frac{1}{n_p} \int \frac{\delta(E^{(0)} + E_{\text{pair}}^{\Delta\text{NO}})}{\delta\chi_p(\mathbf{x})} \chi_q(\mathbf{x}) d\mathbf{x} \quad (30)$$

denotes a generalized  $\Delta\text{NO}$  Fock matrix element, where  $\chi_p(\mathbf{x})$  is a natural spin-orbital. The antisymmetrized electron repulsion integrals are given by  $\langle pq || rs \rangle = \langle pq | rs \rangle - \langle pq | sr \rangle$  with

$$\langle pq | rs \rangle = \int \frac{\chi_p(\mathbf{x}_1) \chi_q(\mathbf{x}_2) \chi_r(\mathbf{x}_1) \chi_s(\mathbf{x}_2)}{r_{12}} d\mathbf{x}_1 d\mathbf{x}_2. \quad (31)$$

Besides introducing occupancies and vacancies, and expanding the range of the sums over spin-orbitals, one more modification is applied to both the  $r_i^a$  and  $r_{ij}^{ab}$  equations. The leading term of each residual equation is multiplied by a damping factor ( $s_i^a$  for  $r_i^a$

and  $d_{ij}^{ab}$  for  $r_{ij}^{ab}$ ), which are defined in the Appendix. The damping factors are derived by considering the difference between the zeroth-order 2-RDM,  $\Gamma^{(0)}$ , and the pair-corrected and statically correlated  $\Delta\text{NO}$  2-RDM,  $\Gamma^{\Delta\text{NO}}$ . The effects of the pair correction are derived for each occupied-occupied, and virtual-virtual, spin-orbital pair and the effects of static correlation and the high-spin correction are derived by considering each statically correlated electron pair.

The CCSD energy expression is unmodified, with the exception of the range of summation,

$$E_{\text{CCSD}}^{\Delta\text{NO}} = \sum_{ia} t_i^a F_{ia} + \frac{1}{2} \sum_{ijab} \left( \frac{t_{ij}^{ab}}{2} - t_i^a t_j^b \right) \langle ij || ab \rangle. \quad (32)$$

### C. MP2 for $\Delta\text{NO}$

An equation for the MP2 amplitudes is derived in a manner analogous to CCSD, where the two instructions of White and Chan (see Subsection II B) are applied to the usual noncanonical MP2 residual equation,

$$r_{ij}^{ab}(\text{MP2}) = n_i n_j h_a h_b d_{ij}^{ab} \langle ij || ab \rangle + \sum_c \left( h_b t_{ij}^{ac} F_{bc} + h_a t_{ij}^{cb} F_{ac} \right) - \sum_k \left( n_j t_{ik}^{ab} F_{jk} + n_i t_{kj}^{ab} F_{ik} \right), \quad (33)$$

where, in addition to the introduction of occupancies and vacancies and the expanded range of summation, the same damping factor (defined in the Appendix) applied to the CCSD  $r_{ij}^{ab}$  equation [see Eq. (26)] is applied here. Also, like CCSD, the MP2 energy expression remains the same with the exception of the expanded range of summation, i.e.,

$$E_{\text{MP2}}^{\Delta\text{NO}} = \frac{1}{4} \sum_{ijab} t_{ij}^{ab} \langle ij || ab \rangle. \quad (34)$$

Note that because the orbital invariant formulation of MP2<sup>67</sup> is employed, Eqs. (33) and (34) do not involve single excitations.

## III. METHOD

### A. FCI reference

Benchmark potential energy curves were obtained using a determinant-driven selected configuration interaction (sCI) method known as CIPSI (Configuration Interaction using a Perturbative Selection made Iteratively)<sup>68–70</sup> in which the energies are extrapolated to the full configuration interaction (FCI) result using multireference perturbation theory.<sup>71–73</sup> The all-electron extrapolated-FCI (exFCI) calculations were performed using Quantum Package 2.0.<sup>73</sup> All benchmark and  $\Delta\text{NO}$  calculations were performed using the cc-pVTZ/f basis set.<sup>74–77</sup>

### B. $\Delta\text{NO}$

All  $\Delta\text{NO}$  and subsequent MP2 and CCSD calculations were performed using the MUNgauss quantum chemistry program.<sup>78</sup> Optimization of  $\{\phi_m\}$  and  $\{\Delta_{me}\}$  was performed according to the previously established algorithm.<sup>8,79</sup> Restricted Hartree-Fock orbitals serve as the initial guess NOs, which are then optimized via iterative

diagonalization of a pseudo-Fock matrix.  $\{\Delta_{me}\}$  are optimized using a Newton-Raphson algorithm. For the current study, the number of active occupied orbitals was chosen manually to be the number of bonds in the diatomic. An equivalent number of virtual orbitals were chosen to be active.

### C. MP2 and CCSD

Both the MP2 and CCSD algorithms are implemented in the spin-orbital basis. The residual equations are solved using an iterative Newton-Raphson (MP2), or approximate Newton-Raphson (CCSD), approach. Amplitude updates are calculated via

$$t_i^a \leftarrow t_i^a + \frac{r_i^a}{n_i F_{ii} - h_a F_{aa}}, \quad (35a)$$

$$t_{ij}^{ab} \leftarrow t_{ij}^{ab} + \frac{r_{ij}^{ab}}{n_i F_{ii} + n_j F_{jj} - h_a F_{aa} - h_b F_{bb}}, \quad (35b)$$

where the initial  $t_{ij}^{ab}$  amplitudes are set to the MP2 values and  $t_i^a = 0$ . To avoid numerical instabilities, residuals,  $r_i^a$  and  $r_{ij}^{ab}$ , are considered to be zero if the leading term [see Eqs. (25) and (26) for CCSD and Eq. (33) for MP2] is below a specific threshold  $\mu$ ,

$$r_i^a = 0, \quad \text{if } n_i h_a d_i^a F_{ia} < \mu, \quad (36a)$$

$$r_{ij}^{ab} = 0, \quad \text{if } n_i n_j h_a h_b d_{ij}^{ab} \langle ij || ab \rangle < \mu. \quad (36b)$$

Here,  $\mu$  is set to machine precision. The iterative optimization of the amplitudes is accelerated using a direct inversion of iterative subspace (DIIS) algorithm<sup>80</sup> to extrapolate from amplitudes of previous steps.<sup>81</sup> A maximum number of 10 sets of amplitudes from previous steps were kept for extrapolation. In the case of the CCSD iterations,  $t_i^a$  and  $t_{ij}^{ab}$  were combined and extrapolated together. Convergence was assumed when the absolute value of the largest residual element was less than  $10^{-7}$ .

## IV. RESULTS

The error in the  $\Delta$ NO-MP2 and  $\Delta$ NO-CCSD potential energy curves,  $U(R)$ , for  $H_2$  compared to exFCI is presented in Fig. 2. The potential energy curve is calculated as

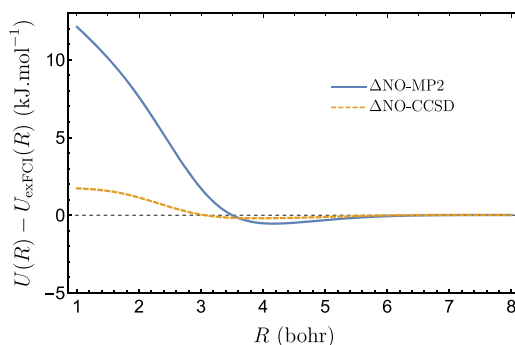


**FIG. 2.** Error (in  $\text{kJ mol}^{-1}$ ) in  $H_2$  potential energy curves compared to exFCI. The error in  $U_{\text{MP2}}(R)$  is  $17 \text{ kJ mol}^{-1}$  at  $R = 1$  bohr and continues to grow with increasing  $R$ . For  $H_2$ ,  $U_{\text{CCSD}}(R) = U_{\text{exFCI}}(R)$ , and therefore, the CCSD error is zero for all  $R$ .

$$U(R) = E(R) + V_{\text{nn}}(R), \quad (37)$$

where the nuclear repulsion energy,  $V_{\text{nn}}(R)$ , is added to the electronic energy obtained from  $\Delta$ NO-MP2,  $\Delta$ NO-CCSD, or exFCI. For  $H_2$ , the exFCI result is equivalent to regular FCI and, hence, the exact result for the given basis set. Also, for two electrons, CCSD is equivalent to FCI, and therefore, any error in  $U_{\Delta\text{NO-CCSD}}(R)$  is due to the manner in which the  $\Delta$ NO static correlation energy is blended with the CCSD dynamic correlation energy. This leads to a maximum error of  $1.7 \text{ kJ mol}^{-1}$  at the beginning of the examined range,  $R = 1$  bohr. There is also a slight overestimation of the total correlation energy at stretched bond lengths, with a maximum deviation of  $-0.2 \text{ kJ mol}^{-1}$  at  $R = 3.89$  bohrs. In the case of  $\Delta$ NO-MP2, the error at small  $R$  is much larger. This can be attributed to the fact that, as  $R \rightarrow 0$ , the correlation energy approaches that of He, for which the MP2 correlation energy differs from the FCI correlation energy by  $15.5 \text{ kJ mol}^{-1}$ . As  $R$  increases, the error in  $U_{\Delta\text{NO-MP2}}(R)$  decreases, also with a slight overestimation of correlation energy ( $-0.5 \text{ kJ mol}^{-1}$  at  $R = 4.17$  bohrs) at stretched bond lengths. For both methods, the damping factors ensure that, as  $R \rightarrow \infty$ , the dynamic correlation energy vanishes, along with the error in  $U(R)$ .

Equilibrium bond lengths and dissociation energies predicted by  $\Delta$ NO-MP2 and  $\Delta$ NO-CCSD for a selection of diatomics are

**TABLE II.** Calculated equilibrium bond lengths  $R_e$  and dissociation energies  $D_e$  for a selection of diatomics.

Molecule	$R_e$ (bohrs)						$D_e$ ( $\text{kJ mol}^{-1}$ )						
	exFCI	MP2	CCSD	$\Delta\text{NO}^a$	$\Delta\text{NO-MP2}$	$\Delta\text{NO-CCSD}$	exFCI	MP2 <sup>c</sup>	CCSD	$\Delta\text{NO}^a$	$\Delta\text{NO-MP2}$	$\Delta\text{NO-CCSD}$	NOF-MP2 <sup>b</sup>
$H_2$	1.405	1.392	1.405	1.428	1.408	1.405	454		454	399	443	452	
LiH	3.028	3.019	3.027	3.019	3.044	3.030	236	343	238	185	223	233	
HF	1.729	1.731	1.725	1.735	1.741	1.741	576	667	641	470	603	606	590
LiF	2.981	2.986	2.976	2.946	2.991	2.979	549	612	610	424	593	582	590
$F_2$	2.692	2.655	2.649	2.779	2.623	2.634	143		268	67	138	148	192
$N_2$	2.083	2.102	2.069	2.071	2.084	2.077	880		780	712	856	891	965

<sup>a</sup>From potential energy curve where  $E_{\text{dyn}}^{\Delta\text{NO}} = 0$ .

<sup>b</sup>Orbital-invariant formulation of NOF-MP2 (NOF-OIMP2/cc-pVTZ) from the work of Piris.<sup>54</sup>

<sup>c</sup> $D_e$  for potential energy curves with singularities are not reported.

compared to  $\Delta\text{NO}$  (no dynamic correlation),  $\text{NOF-MP2}$ ,<sup>54</sup>  $\text{MP2}$ ,  $\text{CCSD}$ , and  $\text{exFCI}$  values in Table II.

As expected from Fig. 2, the  $\text{H}_2$   $R_e$  and  $D_e$  values predicted by  $\Delta\text{NO-MP2}$  and  $\Delta\text{NO-CCSD}$  are very close to the  $\text{exFCI}$  values. The underestimation of  $D_e$  by  $\Delta\text{NO-MP2}$  is attributable to the lack of dynamic correlation at small to intermediate  $R$ . Removal of all of the dynamic correlation, by using  $\Delta\text{NO}$ , results in a much larger underestimation of  $D_e$  (by  $55 \text{ kJ mol}^{-1}$ ). No  $\text{MP2}$   $D_e$  value is reported due to the well-known divergence of the potential energy curve to  $-\infty$  as  $R$  increases. The divergence is due to the degeneracy of the  $\sigma$ -bonding and  $\sigma^*$ -antibonding orbitals of  $\text{H}_2$  as  $R \rightarrow \infty$  and is completely removed in the  $\Delta\text{NO-MP2}$  treatment.

The  $\Delta\text{NO-MP2}$ ,  $\Delta\text{NO-CCSD}$ ,  $\text{MP2}$ ,  $\text{CCSD}$ , and  $\text{exFCI}$  curves for  $\text{LiH}$  are presented in Fig. 3. Both  $\Delta\text{NO-MP2}$  and  $\Delta\text{NO-CCSD}$  provide an accurate model of  $\text{LiH}$  dissociation. Most of the error in  $U_{\Delta\text{NO-MP2}}(R)$  occurs near equilibrium, deviating from  $U_{\text{exFCI}}(R)$  by  $20 \text{ kJ mol}^{-1}$  at  $R = 3.028$  bohrs. However,  $U_{\Delta\text{NO-CCSD}}(R)$  only deviates by  $3 \text{ kJ mol}^{-1}$  at equilibrium and  $0.2 \text{ kJ mol}^{-1}$  near dissociation,  $R = 11$  bohrs. This means both the static correlation of the  $\text{LiH}$  bond and dynamic correlation of the electrons on  $\text{Li}$  are effectively captured by  $\Delta\text{NO-CCSD}$ . Inclusion of only static correlation, via  $\Delta\text{NO}$ , leads to a reasonable prediction of  $R_e$  (3.019 bohrs), but  $D_e$  is underestimated by  $51 \text{ kJ mol}^{-1}$ .

The potential energy curves for  $\text{F}_2$  are shown in Fig. 4, and the error in  $U_{\Delta\text{NO-MP2}}(R)$  and  $U_{\Delta\text{NO-CCSD}}(R)$  compared to  $U_{\text{exFCI}}(R)$  is shown in Fig. 5. Similar to other post-Hartree-Fock correlation methods,  $\Delta\text{NO-MP2}$  and  $\Delta\text{NO-CCSD}$  struggle to capture the dynamic correlation in  $\text{F}_2$  near equilibrium and in the separated F atoms.<sup>70</sup> This is evident in the large separation between the  $\text{exFCI}$  curve and all the others. In the case of  $\Delta\text{NO-MP2}$  and  $\Delta\text{NO-CCSD}$ , the lack of dynamic correlation is relatively consistent, and therefore, the predicted  $D_e$  values are reasonable for both, with  $\Delta\text{NO-MP2}$  differing from  $\text{exFCI}$  by  $-5 \text{ kJ mol}^{-1}$  and  $\Delta\text{NO-CCSD}$  differing by  $+5 \text{ kJ mol}^{-1}$ . The lack of dynamic correlation has a more significant effect on the predicted  $R_e$  values, which differ by  $-0.07$  bohr for  $\Delta\text{NO-MP2}$  and  $-0.06$  bohr for  $\Delta\text{NO-CCSD}$ . This is unsurprising when considering that the error in both  $U_{\Delta\text{NO-MP2}}(R)$  and  $U_{\Delta\text{NO-CCSD}}(R)$  varies the most around  $R_e$  (Fig. 5). The predicted  $R_e$  values from  $\text{MP2}$  and  $\text{CCSD}$  also deviate negatively from the  $\text{exFCI}$   $R_e$ , but the deviation is smaller, approximately  $-0.04$  bohr. If dynamic correlation is completely neglected ( $\Delta\text{NO}$ ),  $R_e$  is significantly overestimated ( $+0.09$  bohr), and the estimated  $D_e$  is exceptionally small,  $67 \text{ kJ mol}^{-1}$ .

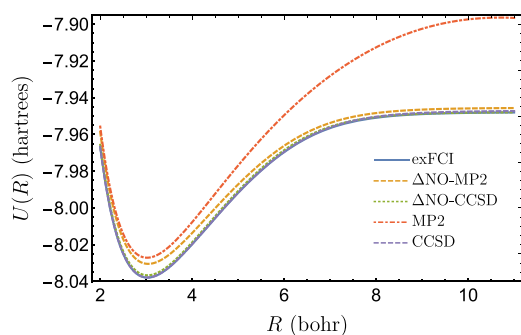


FIG. 3. Calculated  $\text{LiH}$  potential energy curves.

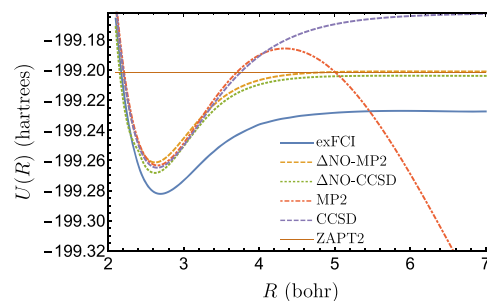


FIG. 4. Calculated  $\text{F}_2$  potential energy curves. The ZAPT2 energy of two separate F atoms is included for comparison.

For a given molecule, the  $\Delta\text{NO}$  energy without dynamic correlation energy (simply referred to as  $\Delta\text{NO}$  in Table II),  $E_{\text{no-dyn}}^{\Delta\text{NO}} = E^{(0)} + E_{\text{pair}}^{\Delta\text{NO}} + E_{\text{stat}}^{\Delta\text{NO}} + E_{\text{HSC}}^{\Delta\text{NO}}$ , is equivalent to the sum of restricted open-shell Hartree-Fock (ROHF) energies at the bond dissociation limit,

$$\lim_{R \rightarrow \infty} E_{\text{no-dyn}}^{\Delta\text{NO}}[\text{A} \cdot \text{R} \cdot \text{B}] = E_{\text{ROHF}}[\text{A}] + E_{\text{ROHF}}[\text{B}]. \quad (38)$$

Therefore, the quality of the  $\Delta\text{NO-MP2}$  treatment near the bond dissociation limit can be assessed through comparison of the  $\Delta\text{NO-MP2}$  energy to the ROHF energy plus the  $z$ -averaged second-order perturbation energy (ZAPT2)<sup>82</sup> of the two separated fragments. The ZAPT2 energy of two F atoms is plotted in Fig. 4, where it is seen that the  $\Delta\text{NO-MP2}$  energy is  $1.0 \text{ kJ mol}^{-1}$  higher. This confirms that  $\Delta\text{NO-MP2}$  is correctly capturing and partitioning the static and dynamic correlation energy of  $\text{F}_2$ . This is in sharp contrast to  $\text{CCSD}$  which drastically overestimates  $D_e$  or  $\text{MP2}$  which diverges due to orbital degeneracy. It is clear that, contrary to conventional single-reference methods such as  $\text{MP2}$  and  $\text{CCSD}$ , the hybrid  $\Delta\text{NO-MP2}$  and  $\Delta\text{NO-CCSD}$  methods proposed here are able to accurately model strongly correlated systems.

Similar to  $\text{F}_2$ , the dynamic correlation of the F atom in  $\text{HF}$  and  $\text{LiF}$  is not sufficiently captured by  $\Delta\text{NO-MP2}$  or  $\Delta\text{NO-CCSD}$ . This leads to overestimation of  $D_e$  compared to  $\text{exFCI}$  (see Table II). However, the lack of static correlation in  $\text{MP2}$  and  $\text{CCSD}$  leads to even larger overestimation of  $D_e$ .

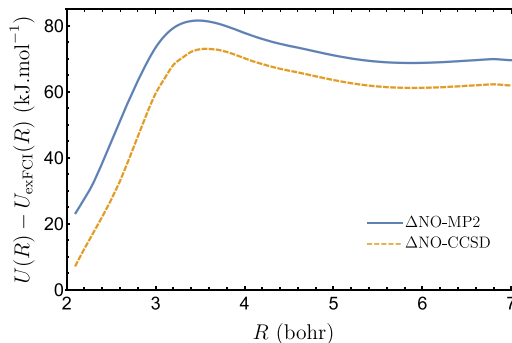
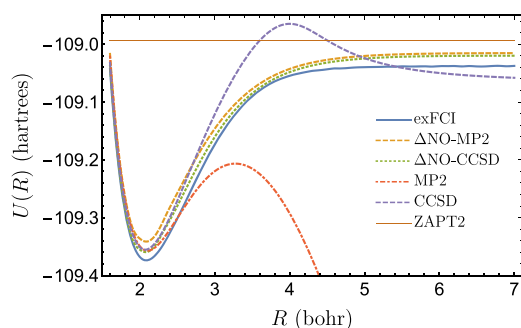


FIG. 5. Error (in  $\text{kJ mol}^{-1}$ ) in  $\text{F}_2$  potential energy curves compared to  $\text{exFCI}$ .



**FIG. 6.** Calculated  $N_2$  potential energy curves. The ZAPT2 energy of two separate N atoms is included for comparison.

In Fig. 6, the  $\Delta$ NO-MP2 and  $\Delta$ NO-CCSD potential energy curves for  $N_2$  are compared to that of MP2, CCSD, and exFCI. The error in  $U_{\Delta\text{NO-MP2}}(R)$  and  $U_{\Delta\text{NO-CCSD}}(R)$  compared to  $U_{\text{exFCI}}(R)$  is also shown in Fig. 7. Like  $F_2$ ,  $\Delta$ NO-MP2 overestimates  $D_e$ , while  $\Delta$ NO-CCSD underestimates it. Albeit, the amount by which the  $\Delta$ NO methods are in error is somewhat greater,  $-24 \text{ kJ mol}^{-1}$  for  $\Delta$ NO-MP2 and  $+11 \text{ kJ mol}^{-1}$  for  $\Delta$ NO-CCSD. Significantly more dynamic correlation is captured by  $\Delta$ NO-CCSD near equilibrium compared to  $\Delta$ NO-MP2. At the exFCI equilibrium bond length,  $R_e = 2.083$  bohrs,  $U_{\Delta\text{NO-CCSD}}(R)$  is  $38 \text{ kJ mol}^{-1}$  above  $U_{\text{exFCI}}(R)$ , whereas  $U_{\Delta\text{NO-MP2}}(R)$  is  $85 \text{ kJ mol}^{-1}$  above. Both predicted equilibrium bond lengths are in good agreement with the exFCI values, particularly the  $\Delta$ NO-CCSD value of  $R_e = 2.084$  bohrs. At dissociation, both methods underestimate the dynamic correlation by similar amounts,  $60 \text{ kJ mol}^{-1}$  for  $\Delta$ NO-MP2 and  $53 \text{ kJ mol}^{-1}$  for  $\Delta$ NO-CCSD. Interestingly, the  $\Delta$ NO-MP2 energy at dissociation is  $58 \text{ kJ mol}^{-1}$  lower than the ZAPT2 result for two separate N atoms. Analysis of the components of the ZAPT2 and  $\Delta$ NO-MP2 correlation energies reveals that it is the correlation between the statically correlated electrons (i.e., unpaired electrons) that is responsible for this difference. This discrepancy, for  $F_2$  and  $N_2$ , suggests that both  $\Delta$ NO-MP2 and  $\Delta$ NO-CCSD are not size-consistent. However, further analysis is required to reveal the origin of, and fully understand, the discrepancy.

For the small collection of molecules studied, the quality of  $\Delta$ NO-MP2 and  $\Delta$ NO-CCSD improves, compared to the

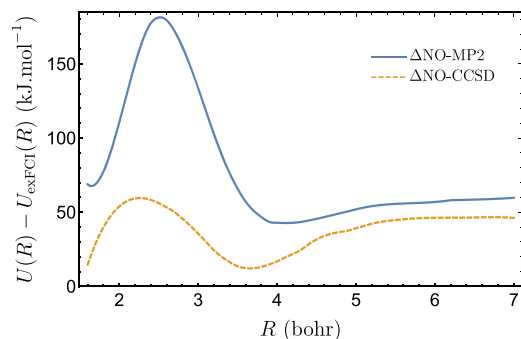


**FIG. 7.** Error (in  $\text{kJ mol}^{-1}$ ) in  $N_2$  potential energy curves compared to exFCI.

single-reference MP2 and CCSD, as the complexity of the system increases. Expectedly, as the amount of static correlation increases (i.e., small  $R$  to large  $R$  or single bond to triple bond), the  $\Delta$ NO methods become significantly superior.

## V. CONCLUSIONS

Combining multireference methods for static correlation with post-Hartree-Fock methods for dynamic correlation is a common approach to modeling complex electronic systems. Despite the noted success of CFT methods in modeling systems with multireference character, there is only one example of using such a method in combination with post-Hartree-Fock correlation, which is NOF-MP2. In this work, a CFT method,  $\Delta$ NO, is combined with both MP2 and CCSD in a fashion completely analogous to each other. This is achieved by incorporating occupancies and vacancies, and expanded domains for occupied and virtual orbitals, according to guidelines used to derive FT-CCSD. Additionally, the MP2 and CCSD correlation energies are combined with  $\Delta$ NO by inserting  $\Delta$ -dependent damping factors into the residual equations. The damping factors are defined by considering the description of statically correlated electron pairs by the  $\Delta$ NO 2-RDM, particularly the spin-orbitals they simultaneously occupy (and vacate) as static correlation becomes appreciable.

For the six diatomics studied, both  $\Delta$ NO-MP2 and  $\Delta$ NO-CCSD predict reasonable bond lengths and dissociation energies compared to the benchmark exFCI values. The error in the descriptions of HF, LiF, and  $F_2$  is largely due to the inability of MP2, or CCSD, to account for all of the dynamic correlation among the electrons of F. The larger error in  $D_e$  values predicted for  $N_2$  is likely due to the fact that three bonds are being broken compared to one in the other diatomics. However, the discrepancy between the  $\Delta$ NO-MP2 energy for dissociated  $N_2$  and the ZAPT2 energy for two N atoms deserves attention. This, in combination with the discrepancy between the CCSD and  $\Delta$ NO-CCSD curves for  $H_2$ , suggests that further analysis of the modified MP2 and CCSD equations, in particular, could lead to a more seamless fusion of  $\Delta$ NO and post-Hartree-Fock methods.

In addition to providing an alternative treatment of multireference systems, the  $\Delta$ NO-MP2 and  $\Delta$ NO-CCSD methods offer insight into static and dynamic correlation and the balance between the two. Although most definitions of static correlation make use of the concept of degeneracy or near-degeneracy, the methods presented here are free from any such arguments. The damping factors are based on the simultaneous occupancy (or vacancy) of active spin-orbitals. The damping factors modify the MP2 and CCSD residual equations according to how the  $\Delta$ NO static correlation influences the 2-RDM. Such concepts are relatively easy to grasp in the limit of complete static correlation and provide a useful “physical” picture of a multireference system.

## ACKNOWLEDGMENTS

J.W.H. thanks the Natural Sciences and Engineering Research Council of Canada (NSERC) for a Discovery Grant, Compute/Calcul Canada for computing resources, the Université Paul Sabatier (Toulouse, France) for a visiting fellowship, and the Discovery Institute for Computation and Synthesis for useful consultations. The authors also thank Anthony Scemama for helpful discussions.

## APPENDIX: AMPLITUDE DAMPING

The MP2 and CCSD equations adopted from the finite-temperature versions (see Subsections II B and II C) are modified for use with the  $\Delta$ NO method by incorporating a single excitation,  $s_i^a$ , and a double excitation,  $d_{ij}^{ab}$ , damping factor. The single excitation damping factor included in the CCSD  $r_i^a$  equation takes a rather simple form,

$$s_i^a = \begin{cases} 0, & \text{if } \phi_i \in \mathcal{A}, \\ 1, & \text{otherwise.} \end{cases} \quad (\text{A1})$$

In other words, all single excitations from the active  $\Delta$ NO orbitals are turned off. This arises from the assumption that single excitations are responsible for orbital relaxation<sup>83,84</sup> and that the most significant part of the active orbital relaxation (due to static correlation) is obtained via the  $\Delta$ NO orbital optimization.

For double excitations, the damping factor,

$$d_{ij}^{ab} = \alpha_{ij} \alpha^{ab} \beta_{ij} \beta^{ab} \beta_i^a \beta_j^b \beta_i^b \beta_j^a, \quad (\text{A2})$$

is composed of pair correction,  $\alpha_{ij} \alpha^{ab}$ , and static correlation and high-spin correction,  $\beta_{ij} \beta^{ab} \beta_i^a \beta_j^b \beta_i^b \beta_j^a$ , contributions. Terms are defined for each possible occupied-virtual pairing,  $\beta_i^a \beta_j^b \beta_i^b \beta_j^a$ , to maintain the symmetry of the amplitudes,  $t_{ij}^{ab} = -t_{ji}^{ab} = -t_{ij}^{ba} = t_{ji}^{ba}$ .

In the double excitation residual equations for both MP2 [Eq. (33)] and CCSD [Eq. (26)], the damping factor is applied to the leading term that includes a product of the orbital occupancies and vacancies,  $n_i n_j h_a h_b$ . The pair-correction contribution to the damping factor,  $\alpha_{ij}$  and  $\alpha^{ab}$ , corrects the occupancy-occupancy and vacancy-vacancy products, respectively. The occupancy-occupancy term is defined as

$$\alpha_{pq} = \frac{(\Gamma^{(0),\uparrow\uparrow})_{pqpq} + (\Gamma_{\text{pair}}^{\Delta\text{NO},\uparrow\uparrow})_{pqpq}}{(\Gamma^{(0),\uparrow\uparrow})_{pqpq}}, \quad (\text{A3})$$

$$\alpha_{p\bar{q}} = \frac{(\Gamma^{(0),\uparrow\downarrow})_{pqpq} + (\Gamma_{\text{pair}}^{\Delta\text{NO},\uparrow\downarrow})_{pqpq}}{(\Gamma^{(0),\uparrow\downarrow})_{pqpq}}.$$

As in the MP2 and CCSD equations, the indices of the damping factors refer to spin-orbitals. In the  $\Delta$ NO method, terms are

labeled according to spatial NOs. Here, the labeling ( $p, q$ ) corresponds to spatial NOs, with spin-orbitals distinguished using an overbar for spin-down orbitals and no overbar for spin-up orbitals. The vacancy-vacancy pair-correction factor,  $\alpha^{ab}$ , is defined in the same manner as that for occupancy-occupancy,  $\alpha_{ij}$ , except all occupancies ( $n_p$ ) are replaced by vacancies ( $h_p$ ), and the sign of  $\Delta$ 's is reversed because they have the opposite effect on vacancies,

$$\alpha^{pq} = \alpha_{pq} \Big|_{\substack{n \rightarrow h \\ \Delta \rightarrow -\Delta}}. \quad (\text{A4})$$

From these equations, expressions for the pair-correction factors for occupancy-occupancy and vacancy-vacancy pairs can be determined, for spin-orbitals from the same NO,

$$\alpha_{p\bar{p}} = \frac{1}{n_p}, \quad \alpha^{p\bar{p}} = \frac{1}{h_p}, \quad (\text{A5})$$

and from different NOs,

$$\alpha_{pq} = \alpha_{p\bar{q}} = \frac{(n_p + \Delta_{pq})(n_q - \Delta_{pq}) - \eta_{pq}}{n_p n_q}, \quad (\text{A6})$$

$$\alpha^{pq} = \alpha^{p\bar{q}} = \frac{(h_p - \Delta_{pq})(h_q + \Delta_{pq}) - \eta_{pq}}{h_p h_q}. \quad (\text{A7})$$

The remaining contribution to the damping factors is from the static correlation and the high-spin correction of the 2-RDM. Each spin-orbital pair contribution is also defined by a ratio of 2-RDM components; however, in this case, the difference between the numerator and the denominator is the contribution from static correlation and the high-spin correction,

$$\beta_{mn} = \frac{G_{mn}^{\Delta\text{NO},\uparrow\uparrow}}{G_{mn}^{(0),\uparrow\uparrow} + (G_{\text{pair}}^{\Delta\text{NO},\uparrow\uparrow})_{mn}}, \quad (\text{A8})$$

$$\beta_{m\bar{n}} = \frac{G_{mn}^{\Delta\text{NO},\uparrow\downarrow}}{G_{mn}^{(0),\uparrow\downarrow} + (G_{\text{pair}}^{\Delta\text{NO},\uparrow\downarrow})_{mn}}.$$

The above definitions only apply to active-occupied spin orbitals (denoted by  $m, \bar{m}, n$ , and  $\bar{n}$ ). These quantities are defined in terms of sums over 2-RDM elements,

$$G_{mn}^{\Delta\text{NO},\uparrow\uparrow} = \sum_{pq} \left( \Gamma_{pqpq}^{\Delta\text{NO},\uparrow\uparrow} \Big|_{\substack{n_k=0 \\ \Delta_{ke}=0 \\ (k \neq m,n)}} - \Gamma_{pqpq}^{\Delta\text{NO},\uparrow\uparrow} \Big|_{\substack{n_k=0 \\ \Delta_{ke}=0 \\ (k \neq m)}} - \Gamma_{pqpq}^{\Delta\text{NO},\uparrow\uparrow} \Big|_{\substack{n_k=0 \\ \Delta_{ke}=0 \\ (k \neq n)}} \right), \quad (\text{A9})$$

$$G_{m\bar{n}}^{\Delta\text{NO},\uparrow\downarrow} = \begin{cases} \sum_{pq} \Gamma_{ppqq}^{\Delta\text{NO},\uparrow\downarrow} \Big|_{\substack{n_k=0 \\ \Delta_{ke}=0 \\ (k \neq m)}}, & \text{if } m = n, \\ \sum_{pq} \left( \Gamma_{pqpq}^{\Delta\text{NO},\uparrow\downarrow} \Big|_{\substack{n_k=0 \\ \Delta_{ke}=0 \\ (k \neq m,n)}} - \Gamma_{pqpq}^{\Delta\text{NO},\uparrow\downarrow} \Big|_{\substack{n_k=0 \\ \Delta_{ke}=0 \\ (k \neq m)}} - \Gamma_{pqpq}^{\Delta\text{NO},\uparrow\downarrow} \Big|_{\substack{n_k=0 \\ \Delta_{ke}=0 \\ (k \neq n)}} \right), & \text{if } m \neq n. \end{cases} \quad (\text{A10})$$

The  $G_{mn}^{\Delta\text{NO},\uparrow\downarrow}$  and  $G_{mn}^{\Delta\text{NO},\uparrow\uparrow}$  terms are defined analogously. By zeroing the contributions of other electron pairs, the sum captures the contributions to the 2-RDM from the electron pairs that originate from the occupied NOs  $m$  and  $n$  only. When  $m \neq n$ , the intrapair contributions are removed. Also notice that the sum over 2-RDM elements is only over the Coulomb-like terms ( $pqpq$ ) for  $m \neq n$  and the time-inversion exchange and Coulomb-like terms for  $m = n$ . These definitions lead to the following expressions for the static correlation and high-spin correction contributions to the damping factors, for active-occupied spin-orbitals:

$$\beta_{m\bar{m}} = \beta_{\bar{m}m} = 1 + \sum_{pq} \sqrt{\Delta_{mp}\Delta_{mq}} - 2 \sum_p \tau_{mp}, \quad (\text{A11})$$

$$\beta_{m\bar{n}} = \beta_{\bar{m}n} = 1 + \zeta_{mn} - 4\kappa_{mn}, \quad (\text{A12})$$

$$\beta_{mn} = \beta_{\bar{m}\bar{n}} = 1 + 4\kappa_{mn}. \quad (\text{A13})$$

In the case of virtual NOs, it is possible that occupancy is transferred from multiple occupied NOs. Therefore, the contributions of static correlation and the high-spin correction to the damping factor are combined through multiplication,

$$\beta_{mf} = \prod_n \beta_{mn}. \quad (\text{A14})$$

The resulting contribution is a product of terms for the electron pairs that are transferred to that particular virtual. If both spin-orbitals are active virtuals, then the product includes all factors for separate electron pairs that are transferred to those virtuals,

$$\beta_{ef} = \prod_{\substack{mn \\ (\Delta_{me} \neq 0) \\ (\Delta_{nf} \neq 0)}} \beta_{mn}. \quad (\text{A15})$$

The vacancy-vacancy contributions are equivalent to the occupancy-occupancy terms,

$$\beta^{pq} = \beta_{pq}. \quad (\text{A16})$$

The intermediate sums,  $G_{mn}^{\Delta\text{NO},\uparrow\uparrow}$  and  $G_{mn}^{\Delta\text{NO},\uparrow\downarrow}$ , are the contribution to the 2-RDM from a particular electron pair. Due to the pair-correction term of the  $\Delta\text{NO}$  2-RDM, the denominator of  $\beta_{mn}$  [Eq. (A8)] is unity,

$$G_{mn}^{(0),\uparrow\uparrow} + \left(G_{\text{pair}}^{\Delta\text{NO},\uparrow\uparrow}\right)_{mn} = G_{m\bar{n}}^{(0),\uparrow\downarrow} + \left(G_{\text{pair}}^{\Delta\text{NO},\uparrow\downarrow}\right)_{m\bar{n}} = 1. \quad (\text{A17})$$

The expressions for  $\beta_{mn}$  and  $\beta_{m\bar{n}}$  can be rewritten accordingly,

$$\begin{aligned} \beta_{mn} &= 1 + \left(G_{\text{stat}}^{\Delta\text{NO},\uparrow\uparrow}\right)_{mn} + \left(G_{\text{HSC}}^{\Delta\text{NO},\uparrow\uparrow}\right)_{mn}, \\ \beta_{m\bar{n}} &= 1 + \left(G_{\text{stat}}^{\Delta\text{NO},\uparrow\downarrow}\right)_{m\bar{n}} + \left(G_{\text{HSC}}^{\Delta\text{NO},\uparrow\downarrow}\right)_{m\bar{n}}. \end{aligned} \quad (\text{A18})$$

The expressions for the occupancy-vacancy damping effect,  $\beta_m^n$  and  $\beta_m^{\bar{n}}$ , can also be written in the same form; however, static correlation and high-spin correction have the opposite effect,

$$\begin{aligned} \beta_m^n &= 1 - \left(G_{\text{stat}}^{\Delta\text{NO},\uparrow\uparrow}\right)_{mn} - \left(G_{\text{HSC}}^{\Delta\text{NO},\uparrow\uparrow}\right)_{mn}, \\ \beta_m^{\bar{n}} &= 1 - \left(G_{\text{stat}}^{\Delta\text{NO},\uparrow\downarrow}\right)_{m\bar{n}} - \left(G_{\text{HSC}}^{\Delta\text{NO},\uparrow\downarrow}\right)_{m\bar{n}}. \end{aligned} \quad (\text{A19})$$

This is due to the inverse nature of vacancy compared to occupancy [i.e., when the spin-up orbital is (locally) occupied, the spin-down orbital is vacant and vice versa]. When applied to spin-orbital pairs involving virtuals, the effects from transferring different electron pairs to that virtual are combined via multiplication,

$$\beta_m^f = \prod_n \beta_m^n, \quad \beta_e^f = \prod_{\substack{mn \\ (\Delta_{me} \neq 0) \\ (\Delta_{nf} \neq 0)}} \beta_m^n. \quad (\text{A20})$$

The above definitions lead to the following expressions for the occupancy-vacancy contributions to the damping factors:

$$\beta_m^{\bar{m}} = 1 - \sum_{pq} \sqrt{\Delta_{mp}\Delta_{mq}} + 2 \sum_p \tau_{mp}, \quad (\text{A21})$$

$$\beta_m^{\bar{n}} = 1 - \zeta_{mn} + 4\kappa_{mn}, \quad \beta_m^n = 1 - 4\kappa_{mn}.$$

Finally, if all indices correspond to active spin-orbitals, then the damping factor is zero, i.e.,

$$\begin{aligned} d_{mn}^{ef} = d_{m\bar{n}}^{e\bar{f}} = d_{m\bar{n}}^{e\bar{f}} = d_{m\bar{n}}^{e\bar{f}} = d_{m\bar{n}}^{e\bar{f}} = d_{m\bar{n}}^{e\bar{f}} = 0, \\ \text{if } \phi_m \wedge \phi_n \wedge \phi_e \wedge \phi_f \in \mathcal{A}. \end{aligned} \quad (\text{A22})$$

It is assumed that such interactions are already included in the  $\Delta\text{NO}$  2-RDM.

## REFERENCES

- D. K. W. Mok, R. Neumann, and N. C. Handy, *J. Phys. Chem.* **100**, 6225 (1996).
- N. C. Handy and A. J. Cohen, *Mol. Phys.* **99**, 403 (2001).
- D. Cremer, *Mol. Phys.* **99**, 1899 (2001).
- A. D. Becke, *J. Chem. Phys.* **138**, 074109 (2013).
- D. L. Crittenden, *J. Phys. Chem. A* **117**, 3852 (2013).
- T. Tsuchimochi and T. V. Voorhis, *J. Chem. Phys.* **141**, 164117 (2014).
- A. J. Wallace and D. L. Crittenden, *J. Phys. Chem. A* **118**, 2138 (2014).
- J. W. Hollett, H. Hosseini, and C. Menzies, *J. Chem. Phys.* **145**, 084106 (2016).
- E. Ramos-Cordoba, P. Salvador, and E. Matito, *Phys. Chem. Chem. Phys.* **18**, 24015 (2016).
- C. L. Benavides-Riveros, N. N. Lathiotakis, and M. A. L. Marques, *Phys. Chem. Chem. Phys.* **19**, 12655 (2017).
- M. Via-Nadal, M. Rodríguez-Mayorga, E. Ramos-Cordoba, and E. Matito, *J. Phys. Chem. Lett.* **10**, 4032 (2019).
- E. Fromager, J. Toulouse, and H. J. Aa. Jensen, *J. Chem. Phys.* **126**, 074111 (2007).
- J. Toulouse, I. C. Gerber, G. Jansen, A. Savin, and J. G. Ángyán, *Phys. Rev. Lett.* **102**, 096404 (2009).
- B. G. Janesko, T. M. Henderson, and G. E. Scuseria, *J. Chem. Phys.* **130**, 081105 (2009).
- J.-D. Chai and M. Head-Gordon, *J. Chem. Phys.* **131**, 174105 (2009).
- A. Stoyanova, A. M. Teale, J. Toulouse, T. Helgaker, and E. Fromager, *J. Chem. Phys.* **139**, 134113 (2013).
- J. Cizek, *Adv. Chem. Phys.* **14**, 35 (1969).
- B. Jeziorski and H. J. Monkhorst, *Phys. Rev. A* **24**, 1668 (1981).
- K. Andersson, P. Malmqvist, B. O. Roos, A. J. Sadlej, and K. Wolinski, *J. Phys. Chem.* **94**, 5483 (1990).
- P. Pulay, *Int. J. Quantum Chem.* **111**, 3273 (2011).
- F. A. Evangelista, *J. Chem. Phys.* **149**, 030901 (2018).

- <sup>22</sup>E. R. Sayfutyarova, Q. Sun, G. K.-L. Chan, and G. Knizia, *J. Chem. Theory Comput.* **13**, 4063 (2017).
- <sup>23</sup>J. J. Bao, S. S. Dong, L. Gagliardi, and D. G. Truhlar, *J. Chem. Theory Comput.* **14**, 2017 (2018).
- <sup>24</sup>P. G. Szalay, T. Müller, G. Gidofalvi, H. Lischka, and R. Shepard, *Chem. Rev.* **112**, 108 (2012).
- <sup>25</sup>D. I. Lyakh, M. Musial, V. F. Lotrich, and R. J. Bartlett, *Chem. Rev.* **112**, 182 (2012).
- <sup>26</sup>A. Köhn, M. Hanauer, L. A. Mück, T.-C. Jagau, and J. Gauss, *Wiley Interdiscip. Rev.: Comput. Mol. Sci.* **3**, 176 (2013).
- <sup>27</sup>K. Andersson, P. Malmqvist, and B. O. Roos, *J. Chem. Phys.* **96**, 1218 (1992).
- <sup>28</sup>T. Shiozaki, W. Györfy, P. Celani, and H.-J. Werner, *J. Chem. Phys.* **135**, 081106 (2011).
- <sup>29</sup>C. Angeli, R. Cimiraglia, S. Evangelisti, T. Leininger, and J. Malrieu, *J. Chem. Phys.* **114**, 10252 (2001).
- <sup>30</sup>C. Angeli, R. Cimiraglia, and J. Malrieu, *Chem. Phys. Lett.* **350**, 297 (2001).
- <sup>31</sup>C. Angeli, R. Cimiraglia, and J. Malrieu, *J. Chem. Phys.* **117**, 9138 (2002).
- <sup>32</sup>M. Hoffmann and Y. G. Khait, *Chem. Phys. Lett.* **311**, 372 (1999).
- <sup>33</sup>D. I. Lyakh, V. V. Ivanov, and L. Adamowicz, *J. Chem. Phys.* **122**, 024108 (2005).
- <sup>34</sup>A. J. W. Thom and M. Head-Gordon, *J. Chem. Phys.* **131**, 124113 (2009).
- <sup>35</sup>S. R. Yost, T. Kowalczyk, and T. Van Voorhis, *J. Chem. Phys.* **139**, 174104 (2013).
- <sup>36</sup>E. J. Sundstrom and M. Head-Gordon, *J. Chem. Phys.* **140**, 114103 (2014).
- <sup>37</sup>H. G. A. Burton and A. J. W. Thom, *J. Chem. Theory Comput.* **15**, 4851–4861 (2019).
- <sup>38</sup>T. L. Gilbert, *Phys. Rev. B* **12**, 2111 (1975).
- <sup>39</sup>G. Zumbach and K. Maschke, *J. Chem. Phys.* **82**, 5604 (1985).
- <sup>40</sup>W. Kutzelnigg, *J. Chem. Phys.* **125**, 171101 (2006).
- <sup>41</sup>A. Y. Sokolov and H. F. Schaefer III, *J. Chem. Phys.* **139**, 204110 (2013).
- <sup>42</sup>L. M. Mentel, R. van Meer, O. V. Gritsenko, and E. J. Baerends, *J. Chem. Phys.* **140**, 214105 (2014).
- <sup>43</sup>R. van Meer, O. V. Gritsenko, and E. J. Baerends, *J. Chem. Phys.* **148**, 104102 (2018).
- <sup>44</sup>C. Schilling, *J. Chem. Phys.* **149**, 231102 (2018).
- <sup>45</sup>J. Schmidt, C. L. Benavides-Riveros, and M. A. L. Marques, *Phys. Rev. B* **99**, 224502 (2019).
- <sup>46</sup>A. M. K. Müller, *Phys. Lett. A* **105**, 446 (1984).
- <sup>47</sup>S. Goedecker and C. J. Umrigar, *Phys. Rev. Lett.* **81**, 866 (1998).
- <sup>48</sup>D. R. Rohr, K. Pernal, O. V. Gritsenko, and E. J. Baerends, *J. Chem. Phys.* **129**, 164105 (2008).
- <sup>49</sup>M. Piris and P. Otto, *Int. J. Quantum Chem.* **94**, 317 (2003).
- <sup>50</sup>P. Leiva and M. Piris, *J. Chem. Phys.* **123**, 214102 (2005).
- <sup>51</sup>M. Piris, *Int. J. Quantum Chem.* **113**, 620 (2012).
- <sup>52</sup>M. Piris, *J. Chem. Phys.* **141**, 044107 (2014).
- <sup>53</sup>M. Piris, *Phys. Rev. Lett.* **119**, 063002 (2017).
- <sup>54</sup>M. Piris, *Phys. Rev. A* **98**, 022504 (2018).
- <sup>55</sup>J. T. Margraf and R. Bartlett, *J. Chem. Phys.* **148**, 221103 (2018).
- <sup>56</sup>F. Hummel, *J. Chem. Theory Comput.* **14**, 6505 (2018).
- <sup>57</sup>A. F. White and G. K.-L. Chan, *J. Chem. Theory Comput.* **14**, 5690 (2018).
- <sup>58</sup>G. Sanyal, S. H. Mandal, and D. Mukherjee, *Chem. Phys. Lett.* **192**, 55 (1992).
- <sup>59</sup>G. Sanyal, S. H. Mandal, S. Guba, and D. Mukherjee, *Phys. Rev. E* **48**, 3373 (1993).
- <sup>60</sup>S. H. Mandal, R. Ghosh, G. Sanyal, and D. Mukherjee, *Int. J. Mod. Phys. B* **17**, 5367 (2003).
- <sup>61</sup>M. Kobayashi and T. Taketsugu, *Theor. Chem. Acc.* **134**, 107 (2015).
- <sup>62</sup>R. Santra and J. Schirmer, *Chem. Phys.* **482**, 355 (2017).
- <sup>63</sup>W. Kutzelnigg and D. Mukherjee, *J. Chem. Phys.* **110**, 2800 (1999).
- <sup>64</sup>L. Bytautas, T. M. Henderson, C. A. Jiménez-Hoyos, J. K. Ellis, and G. E. Scuseria, *J. Chem. Phys.* **135**, 044119 (2011).
- <sup>65</sup>W. Polemans, M. Van Raemdonck, B. Verstichel, S. De Baerdemacker, A. Torre, L. Lain, G. E. Massaccesi, D. R. Alcoba, P. Bultinck, and D. Van Neck, *J. Chem. Theory Comput.* **11**, 4064 (2015).
- <sup>66</sup>J. F. Stanton, J. Gauss, J. D. Watts, and R. J. Bartlett, *J. Chem. Phys.* **94**, 4334 (1991).
- <sup>67</sup>P. Pulay and S. Saebø, *Theor. Chim. Acta* **69**, 357 (1986).
- <sup>68</sup>B. Huron, J.-P. Malrieu, and P. Rancurel, *J. Chem. Phys.* **58**, 5745 (1973).
- <sup>69</sup>E. Giner, A. Scemama, and M. Caffarel, *Can. J. Chem.* **91**, 879 (2013).
- <sup>70</sup>E. Giner, A. Scemama, and M. Caffarel, *J. Chem. Phys.* **142**, 044115 (2015).
- <sup>71</sup>Y. Garniron, A. Scemama, P.-F. Loos, and M. Caffarel, *J. Chem. Phys.* **147**, 034101 (2017).
- <sup>72</sup>P.-F. Loos, A. Scemama, A. Blondel, Y. Garniron, M. Caffarel, and D. Jacquemin, *J. Chem. Theory Comput.* **14**, 4360 (2018).
- <sup>73</sup>Y. Garniron, K. Gasperich, T. Applencourt, A. Benali, A. Ferte, J. Paquier, B. Pradines, R. Assaraf, P. Reinhardt, J. Toulouse, P. Barbaresco, N. Renon, G. David, J. P. Malrieu, M. Veril, M. Caffarel, P. F. Loos, E. Giner, and A. Scemama, *J. Chem. Theory Comput.* **15**, 3591 (2019).
- <sup>74</sup>T. H. Dunning, Jr., *J. Chem. Phys.* **90**, 1007 (1989).
- <sup>75</sup>B. P. Prascher, D. E. Woon, K. A. Peterson, T. H. Dunning, and A. K. Wilson, *Theor. Chem. Acc.* **128**, 69 (2011).
- <sup>76</sup>D. Feller, *J. Comput. Chem.* **17**, 1571 (1996).
- <sup>77</sup>K. L. Schuchardt, B. T. Didier, T. Elsethagen, L. Sun, V. Gurumoorthi, J. Chase, J. Li, and T. L. Windus, *J. Chem. Inf. Model.* **47**, 1045 (2007).
- <sup>78</sup>R. A. Poirier, J. W. Hollett, and P. L. Warburton, MUNgauss, Chemistry Department, Memorial University, St. John's, NL, 2015, with contributions from A. Alrawashdeh, J.-P. Becker, J. Besaw, S. D. Bungay, F. Colonna, A. El-Sherbiny, T. Gosse, D. Keefe, A. Kelly, D. Nippard, C. C. Pye, D. Reid, K. Saputantri, M. Shaw, M. Staveley, O. Stueker, Y. Wang, and J. Xidos.
- <sup>79</sup>M. Piris and J. M. Ugalde, *J. Comput. Chem.* **30**, 2078 (2009).
- <sup>80</sup>P. Pulay, *J. Comput. Chem.* **3**, 556 (1982).
- <sup>81</sup>G. E. Scuseria, T. J. Lee, and H. F. Schaefer III, *Chem. Phys. Lett.* **130**, 236 (1986).
- <sup>82</sup>T. J. Lee and D. Jayatilaka, *Chem. Phys. Lett.* **201**, 1 (1993).
- <sup>83</sup>G. E. Scuseria and H. F. Schaefer, *Chem. Phys. Lett.* **142**, 354 (1987).
- <sup>84</sup>C. D. Sherrill, A. I. Krylov, E. F. C. Byrd, and M. Head-Gordon, *J. Chem. Phys.* **109**, 4171 (1998).